

Cite this: *Chem. Sci.*, 2016, 7, 1016

## Co-delivery of nitric oxide and antibiotic using polymeric nanoparticles†

Thuy-Khanh Nguyen,<sup>a</sup> Ramona Selvanayagam,<sup>a</sup> Kitty K. K. Ho,<sup>b</sup> Renxun Chen,<sup>b</sup> Samuel K. Kutty,<sup>b</sup> Scott A. Rice,<sup>cd</sup> Naresh Kumar,<sup>b</sup> Nicolas Barraud,<sup>\*ce</sup> Hien T. T. Duong‡\*<sup>a</sup> and Cyrille Boyer\*<sup>a</sup>

The rise of hospital-acquired infections, also known as nosocomial infections, is a growing concern in intensive healthcare, causing the death of hundreds of thousands of patients and costing billions of dollars worldwide every year. In addition, a decrease in the effectiveness of antibiotics caused by the emergence of drug resistance in pathogens living in biofilm communities poses a significant threat to our health system. The development of new therapeutic agents is urgently needed to overcome this challenge. We have developed new dual action polymeric nanoparticles capable of storing nitric oxide, which can provoke dispersal of biofilms into an antibiotic susceptible planktonic form, together with the aminoglycoside gentamicin, capable of killing the bacteria. The novelty of this work lies in the attachment of NO-releasing moiety to an existing clinically used drug, gentamicin. The nanoparticles were found to release both agents simultaneously and demonstrated synergistic effects, reducing the viability of *Pseudomonas aeruginosa* biofilm and planktonic cultures by more than 90% and 95%, respectively, while treatments with antibiotic or nitric oxide alone resulted in less than 20% decrease in biofilm viability.

Received 29th July 2015  
Accepted 24th October 2015

DOI: 10.1039/c5sc02769a

www.rsc.org/chemicalscience

### Introduction

Nosocomial infections are the fourth leading cause of disease in the U.S.A. and Europe with over 3.5 million cases annually,<sup>1</sup> resulting in significant increases in healthcare costs. More importantly, the number of cases (and by consequence deaths) is rapidly increasing due to the emergence of bacteria resistant to antibiotics.<sup>2,3</sup> One key adaptive process used by bacteria that leads to their survival and development of resistance after antibiotic treatments is the ability to form multicellular communities of cells encased in a matrix of secreted polymeric substances known as microbial biofilms.<sup>4</sup> Their formation and persistence have a considerable impact for patient health, as

many biofilm infections are difficult to resolve, and often result in chronic or recurrent infections.<sup>5-7</sup> Indeed, bacteria in biofilms show significantly increased resistance to external stresses, including antimicrobials and host immune defenses, compared with free-living single bacterial cells.<sup>8,9</sup> Biofilms can also favor gene transfer between bacteria, thus spreading antibiotic resistance or converting a previously non-virulent commensal organism into a virulent pathogen.<sup>10</sup> Consequently, biofilm infections present a number of clinical challenges,<sup>11-17</sup> including diseases involving uncultivable species, chronic inflammation, impaired wound healing, rapidly acquired antibiotic resistance, and the spread of infections. Accordingly, there is an urgent need for novel therapeutics and treatment strategies that are effective against biofilms and biofilm-related infections.

Biofilm researchers have now established that most bacteria follow a lifecycle in which the biofilm mode of growth is the main phase. Bacterial cells can alternate between the biofilm and the planktonic lifestyles *via* transition stages of either attachment or dispersal that involve the expression of specific genes and are highly regulated.<sup>18</sup> In 2006, the biologically ubiquitous nitric oxide (NO) gas was found to be a major signal for biofilm dispersal in the important human pathogen *Pseudomonas aeruginosa*,<sup>19,20</sup> which was found to account for up to 30% of hospital-acquired infectious diseases (nosocomial).<sup>21</sup> Follow-up studies showed that exposure to NO in the pM and low nM range can induce dispersal in several other single- and

<sup>a</sup>Centre for Advanced Macromolecular Design (CAMD) and Australian Centre for NanoMedicine (ACN), School of Chemical Engineering, UNSW Australia, Sydney, NSW 2052, Australia. E-mail: cboyer@unsw.edu.au; hien.duong@sydney.edu.au

<sup>b</sup>School of Chemistry, UNSW Australia, Sydney, NSW 2052, Australia

<sup>c</sup>Centre for Marine-Innovation, School of Biological, Earth and Environmental Sciences, University of New South Wales, Sydney, Australia 2052. E-mail: n.barraud@melix.org

<sup>d</sup>The Singapore Centre for Environmental Life Sciences Engineering and The School of Biological Sciences, Nanyang Technological University, Singapore

<sup>e</sup>Department of Microbiology, Genetics of Biofilms Unit, Institute Pasteur, Paris, France

† Electronic supplementary information (ESI) available: NMR spectra, SEC traces, FTIR, UV-Vis spectra, NO release using amperometric measurement (Fig. S1–S11) are available free of charge *via* the internet. See DOI: 10.1039/c5sc02769a

‡ Present address: School of Chemistry, University of Sydney, Sydney, NSW 2052, Australia.





### Conjugation of POEGMA-*b*-PVBA to gentamicin

Gentamicin sulfate (Enzo Life Sciences, Sapphire Bioscience Pty. Ltd., Australia) ( $0.3 \text{ g}$ ,  $2.02 \times 10^{-4} \text{ mol}$ ) and  $100 \mu\text{L}$  triethylamine (TEA) were dissolved in  $2.5 \text{ mL}$  of distilled water. The solution was left in an incubator at  $37^\circ\text{C}$  whilst being shaken at  $140 \text{ rpm}$  for  $1 \text{ h}$ . Upon completion, drug solution was added into  $2.5 \text{ mL}$  of POEGMA-*b*-PVBA ( $0.3 \text{ g}$ ,  $2.04 \times 10^{-5} \text{ mol}$ ) in distilled water and the mixture of polymer and drug was incubated at  $37^\circ\text{C}$  with shaking at  $100 \text{ rpm}$  for a further  $48 \text{ h}$ . The mixture was then precipitated in acetonitrile and centrifuged at  $7500 \text{ rpm}$  for  $5 \text{ min}$  to remove unreacted gentamicin and salt formed. The supernatant was collected and the precipitation step in acetonitrile was repeated three times. Anhydrous magnesium sulfate was used as a drying agent to remove water from the mixture for further reaction with NO gas to introduce the NO-releasing NONOate moiety to the polymer–drug conjugates in acetonitrile.

### Attachment of NONOate to conjugated POEGMA-*b*-PVBA with gentamicin

The conjugated POEGMA-*b*-PVBA with gentamicin ( $0.3 \text{ g}$ ) was dissolved in acetonitrile ( $5 \text{ mL}$ ) and placed in a Parr apparatus and clamped. The apparatus was then purged and evacuated with nitrogen three times and pressurized to  $5 \text{ atm}$  NO at  $25^\circ\text{C}$  for  $48 \text{ h}$  to form NONOate NO donors. Excess NO was then vented through purging with nitrogen gas. The NONOate polymer was then stored at  $4^\circ\text{C}$  until required for further analysis.

### Determination of NO release by Griess assay and amperometric measurement

NO released from the polymer at specified time intervals was determined using a standard Griess reagent kit (G-7921, Molecular Probes), which is normally used for nitrite determination. NONOate readily releases NO upon contact with water at physiological pH. Typically,  $10 \text{ mg}$  gentamicin-NONOate containing polymer sample was dissolved in  $2 \text{ mL}$  of phosphate-buffered saline (PBS). The solution was enclosed in a sealed dialysis membrane (Cellu-Sep 3500 MWCO) that allows free diffusion of NO. The membrane was then immersed in a  $6 \text{ mL}$  PBS solution and incubated at  $37^\circ\text{C}$  for up to  $24 \text{ h}$ . At various time points, a  $100 \mu\text{L}$  aliquot from the PBS solution was taken for determining concentration of NO. Since NO readily oxidises to nitrite and nitrate upon contact with water, first the reduction of nitrate to nitrite was conducted through a nitrate reductase. For each  $100 \mu\text{L}$  of sample,  $12.5 \mu\text{L}$  of nitrate reductase and  $12.5 \mu\text{L}$  of enzyme cofactor were added into the solution and incubated at room temperature for  $30 \text{ min}$ . Then,  $120 \mu\text{L}$  of Griess reagents was added to the sample and left to incubate at room temperature for  $30 \text{ min}$ . The sample was then topped up with  $395 \mu\text{L}$  of distilled water to make up a total volume of  $640 \mu\text{L}$ . The preparation procedure was repeated for samples at different time points. The UV-Vis absorbance of the resulting solutions was determined at  $548 \text{ nm}$  and the total nitrite concentration in the sample solutions at different time points

were calculated from a standard curve and converted to cumulative NO release.

NO was detected amperometrically by using a TBR4100 free radical analyzer with Lab-Trax-4 digital recorder (World Precision Instruments, Sarasota, USA) and fitted with an NO specific sensor (ISO-NOP). The NO sensor, which was freshly calibrated using *S*-nitroso-*N*-acetylpenicillamine (SNAP) and copper sulfate according to the manufacturer's instructions, was immersed in a vial containing  $10 \text{ mL}$  PBS (pH 7.4) and continuously stirred at  $37^\circ\text{C}$ . After the baseline had stabilized,  $100 \mu\text{L}$  of  $100 \text{ mM}$  gentamicin-NONOate containing polymer solution was added into the vial and instantaneous NO levels were monitored over  $3.5 \text{ h}$ . After this time,  $50 \mu\text{L}$  of a  $50 \text{ mM}$  solution of the free radical scavenger 2-phenyl-4,4,5,5-tetramethylimidazole-1-oxyl-3-oxide (PTIO) was injected into the vial in order to confirm that the amperometric signals being observed were due to NO.

### Analytical instruments

**$^1\text{H-NMR}$  spectroscopy.** Monomer conversions and polymer compositions were analyzed by  $^1\text{H-NMR}$  using a Bruker AC300F ( $300 \text{ MHz}$ ) spectrometer and a Bruker DPX300 ( $300 \text{ MHz}$ ) spectrometer.

OEGMA monomer conversion was determined *via*  $^1\text{H-NMR}$  spectroscopy by the following equation:  $\alpha^{\text{OEGMA}} = 1 - (\int_{5.6 \text{ ppm}} / (\int_{4.1 \text{ ppm}} / 2))$ , where  $\int$  is the peak integral of monomer (vinyl proton at  $5.6 \text{ ppm}$ ,  $1\text{H}$ ) and the polymer (ester proton at  $4.1 \text{ ppm}$ ,  $2\text{H}$ ).

The experimental  $M_{n, \text{NMR}}$  was calculated by using the dithiobenzoate end group peak (*i.e.*  $7.8 \text{ ppm}$ ) in the  $^1\text{H-NMR}$  as a reference, as follows:

$$M_{n, \text{NMR}} = (\int_{4.1 \text{ ppm}} / 2) / (\int_{7.8 \text{ ppm}}) \times M_{w, \text{OEGMA}} + M_{w, \text{CPADB}} \cdot \int_{4.1 \text{ ppm}}$$

and  $\int_{7.8 \text{ ppm}}$  represent the peak integral of OEGMA peak at  $4.1 \text{ ppm}$  ( $2\text{H}$ ) and the dithiobenzoate peak ( $1\text{H}$ ) at  $7.8 \text{ ppm}$ , respectively.  $M_{w, \text{OEGMA}}$  and  $M_{w, \text{CPADB}}$  represent the molar mass of OEGMA and CPADB, respectively.

VBA conversion was calculated from  $^1\text{H NMR}$  spectrum of the reaction mixture using the following equation:  $\alpha^{\text{OEGMA}} = \int_{9.8 \text{ ppm}} / (\int_{10.0 \text{ ppm}} + \int_{9.8 \text{ ppm}})$ , where  $\int_{9.8 \text{ ppm}}$  and  $\int_{10.0 \text{ ppm}}$  correspond to the integrals of aldehyde protons of poly(vinylbenzaldehyde) and vinyl benzaldehyde monomer, respectively.

NMR molecular weight was calculated according to  $M_{n, \text{NMR}} = ((\int_{9.8 \text{ ppm}} / (\int_{4.1 \text{ ppm}} / 2)) \times DP_n^{\text{OEGMA}}) \times M_{w, \text{VBA}} + M_{n, \text{POEGMA macroRAFT}}$ , where  $M_{w, \text{VBA}}$  and  $M_{n, \text{POEGMA macroRAFT}}$  are the molecular weight of monomer and macro RAFT agent, respectively.

In addition,  $^1\text{H NMR}$  spectroscopy was used to demonstrate the conjugation of gentamicin drug to polymers as well as its release in acidic and neutral media, by monitoring changes in the signal at  $9.8 \text{ ppm}$ .

**Size exclusion chromatography (SEC).** SEC analyses of polymer samples were performed in *N,N'*-dimethylacetamide [DMAc with  $0.03\% \text{ w/v}$  LiBr and  $0.05\% \text{ 2,6-di-butyl-4-methylphenol (BHT)}$ ] at  $50^\circ\text{C}$  at flow rate of  $1 \text{ mL min}^{-1}$  with a Shimadzu modular system comprising an SIL-10AD automatic injector,





components were mixed thoroughly in 1 mL of PBS, then 0.3 mL of this solution was trapped between the sample and the glass microscopy slide and allowed to incubate at room temperature in the dark for 20 min. The samples were observed with an Olympus FV1000 Confocal Inverted Microscope, and imaged with a Leica DFC 480 camera. Cells that were stained green were considered to be viable, those that stained red and stained both green and red were considered to be non-viable.

### Statistical analysis

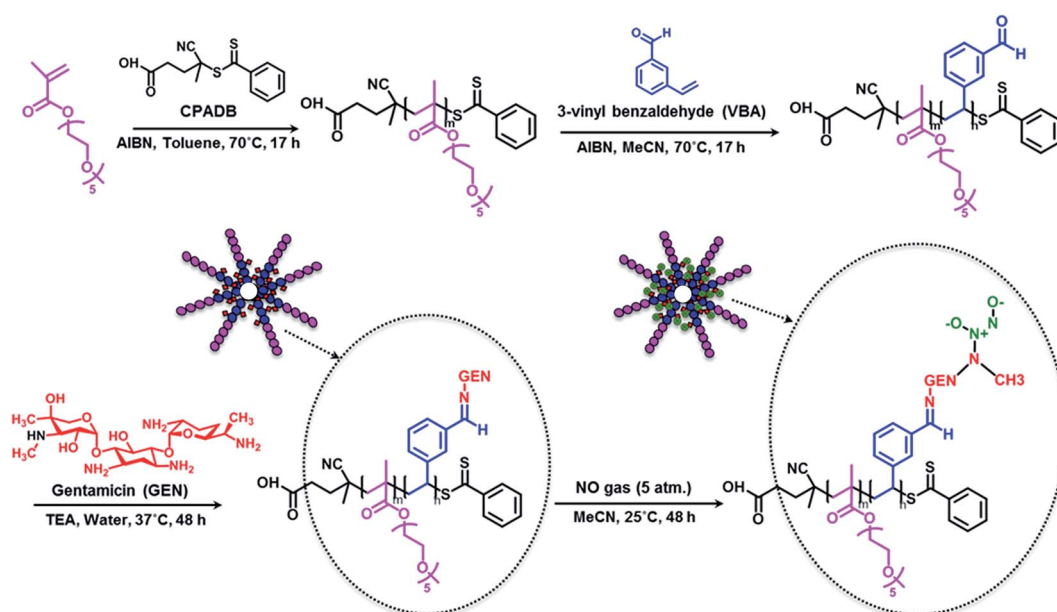
All assays included 2 replicates and were repeated in 2 independent experiments. Statistical analyses were performed with GraphPad Prism 6 (GraphPad Software) using one-way ANOVA followed by Dunnett's multiple comparison test comparing treated samples to the untreated control.

## Results and discussion

In this study, we designed polymeric nanoparticles for the co-delivery of nitric oxide and an antibiotic, gentamicin. To achieve a controlled release of gentamicin, we conjugated gentamicin to the polymer *via* a hydrolysable Schiff base linkage by reacting amino groups of gentamicin (GEN) with aldehyde groups. Aldehyde groups can react rapidly with primary amines to yield a hydrolysable linkage,<sup>36,62–66</sup> that allows a slow release of antibiotic in the middle acidic microenvironment of biofilm.<sup>67,68</sup> To confer water solubility to the polymers, we prepared an amphiphilic block copolymer, constituted of a hydrophilic block (POEGMA), which is closely related to polyethylene glycol leading to excellent biocompatibility, and a short hydrophobic block containing aldehyde groups (PVBA) for further conjugation with gentamicin.

### Synthesis of POEGMA-*b*-PVBA block copolymer

Block copolymer POEGMA-*b*-PVBA was synthesized using living polymerization (*i.e.* reversible addition fragmentation chain transfer (RAFT) polymerization (Scheme 1). Poly((oligoethylene glycol) methyl ether methacrylate) (POEGMA) macro-RAFT agent was prepared in toluene at 70 °C in the presence of 4-cyanopentanoic acid dithiobenzoate (CPADB) as a RAFT agent and oligo(ethylene glycol) methacrylate (OEGMA) as monomer. The monomer conversion was monitored *via* <sup>1</sup>H NMR spectroscopy by comparing the vinyl proton signals (at 6.1 and 5.6 ppm) with ester -OCH<sub>2</sub> proton peaks (at 4.1 ppm). At ~80% monomer conversion, the polymerization was stopped to avoid the formation of significant dead polymers; then, the polymer product was purified by several precipitations (three times) in petroleum spirits. The molecular weight obtained by SEC analysis is in good agreement with the theoretical value ( $M_{n, \text{theo}} = 10\,800 \text{ g mol}^{-1}$ ,  $M_{n, \text{SEC}} = 11\,200 \text{ g mol}^{-1}$ , PDI = 1.08). Subsequently, POEGMA was successfully chain extended in the presence of 3-vinylbenzaldehyde (VBA) to afford POEGMA-*b*-PVBA block copolymer. The conversion of VBA was determined to be around 50% using the vinyl signals at 5.0–6.0 ppm and aromatic signals at 6.5–7.5 ppm (ESI, Fig. S1†) to yield POEGMA-*x*-*b*-VBA<sub>y</sub>, with *x* and *y* equal to 36 and 7. After purification, SEC analysis confirmed the successful chains extension by the molecular weight distribution shift to higher molecular weight ( $M_{n, \text{SEC}} = 13\,700 \text{ g mol}^{-1}$ ) and a low polydispersity index (PDI = 1.13) was obtained (ESI, Fig. S2†). <sup>1</sup>H NMR and FTIR spectroscopy confirmed VBA incorporation by the presence of characteristic signals at 9.8 ppm and at 1710 cm<sup>-1</sup> attributed to aldehyde group, respectively. The final copolymer was constituted by a longer block of OEGMA (36 units) to confer good solubility in water, and a shorter block of VBA (7 units) for functionality. This composition appears ideal to afford well-



Scheme 1 Schematic approach for the preparation of gentamicin-NONOate nanoparticles *via* RAFT polymerization.





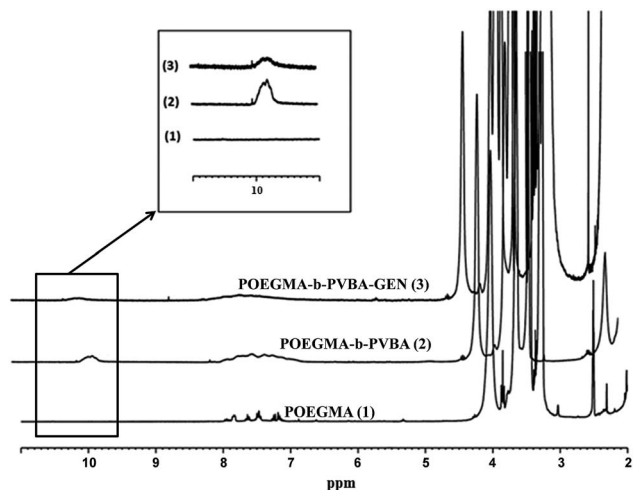


Fig. 2  $^1\text{H}$  NMR spectra of purified POEGMA-*b*-PVBA-GEN overlaid with POEGMA-*b*-PVBA and POEGMA.

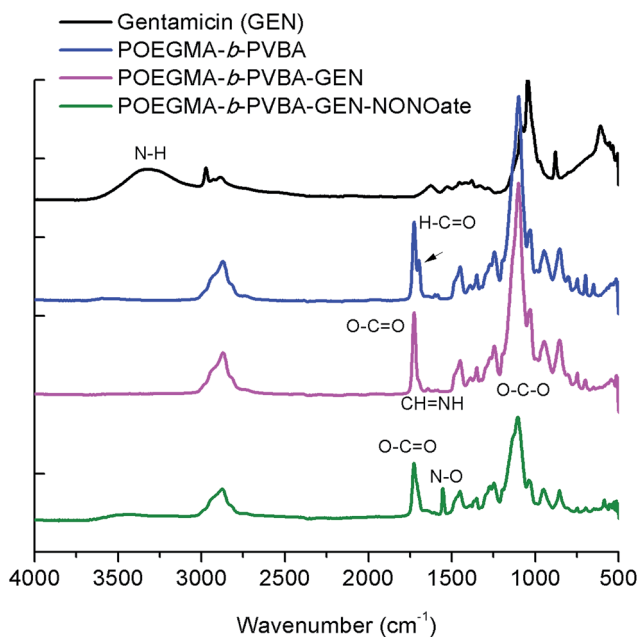


Fig. 3 ATR-FTIR spectra of POEGMA-*b*-PVBA-GEN-NONOate compared with POEGMA-*b*-PVBA-GEN, POEGMA-*b*-PVBA and gentamicin.

bacteria in planktonic form. Our approach was to develop a compound that could disperse the biofilm, thereby making the bacteria more susceptible to antimicrobial agents, and then simultaneously treat the planktonic bacteria. In this study, gentamicin was chosen for this dual purpose owing to the presence of both primary and secondary amine groups. These functional groups allow for an easy conjugation of gentamicin to aldehyde functionalized polymers and the formation of gentamicin-*N*-diazeniumdiolate (gentamicin-NONOate) conjugated polymers by reaction of the secondary amine with nitric oxide (NO) gas. This is a novel approach, which combines the benefit of NO to the existing antibiotics. The NONOate group in

gentamicin-NONOate complex can slowly release NO to regenerate native gentamicin. As gentamicin contains one secondary amine group, theoretically, one NONOate group could be attached per gentamicin. After purification, the polymeric nanoparticles were analyzed by three different techniques: UV-Vis spectroscopy, elemental analysis and ATR-FTIR. Firstly, UV-Vis was performed to quantify the amount of NONOate group by comparing the signal centered at 250 nm (ESI, Fig. S6<sup>†</sup>) before and after NO treatment using molar extinction coefficient for NONOate of  $8500 \text{ M}^{-1} \text{ cm}^{-1}$ .<sup>59,72</sup> The UV-Vis after NO treatment shows an increased signal at around 250 nm, which demonstrates the successful attachment of NO. The amount of NONOate calculated by UV-Vis was close to one NONOate per gentamicin, which is in agreement with the expected values, *i.e.* 3 NONOate per polymer chain. Secondly, elemental analysis was carried out to quantify the amount of nitrogen. After NO treatment, we observed a significant increase of nitrogen (ESI, Table S2<sup>†</sup>), which corresponds to one NONOate per gentamicin, *i.e.* 3 NONOate per polymer chain. Both UV and elemental results are in good agreement. Finally, ATR-FTIR analysis confirmed the presence of the N-O band at  $1510 \text{ cm}^{-1}$  (Fig. 3), indicating the successful attachment of the NONOate group on gentamicin.

#### Determination of gentamicin and nitric oxide release

The imine bond has previously been employed by our group and others for drug conjugation<sup>62–66,69,70</sup> owing to its ability to slowly hydrolyze, which allows a sustainable release of therapeutic compounds. Bacterial biofilms and infected tissue by bacteria usually present a slight acidic pH (typically between 5.5–7.2), which should favor the release of gentamicin from the nanoparticles.<sup>68,73</sup> Gentamicin conjugated nanoparticles were incubated in both pH 7.4 (phosphate buffer) and pH 5.5 (acetate buffer) (ESI, Fig. S7 and S8<sup>†</sup>). Nanoparticles were placed in a dialysis membrane with MWCO 3500 Da and the samples were taken at different time points for gentamicin and NO release. The gentamicin release kinetic from POEGMA-*b*-PVBA nanoparticles was monitored by comparing the aldehyde proton -CHO peak at 9.8 ppm and the -CH<sub>2</sub>O-proton peaks at 4.1 ppm using  $^1\text{H}$  NMR analysis. As expected, the intensity of the signal at 9.8 ppm increased over time, indicating the release of gentamicin. The release rate of gentamicin at pH 5.5 was slightly faster than at pH 7.4. After 17 h, around 50% of gentamicin had been released in both pH values (ESI, Fig. S9<sup>†</sup>). The slow release of gentamicin is desirable as it allows a prolonged action for a long treatment. Concurrently with the release of the gentamicin, the cross-linked structure disassembled into free block copolymer as shown by a decrease of molecular weight by SEC (ESI, Fig. S4 and Table S1<sup>†</sup>).

NO release from GEN-NO nanoparticles was assessed by the Griess assay, which is commonly employed to monitor the cumulative release of NO by several groups<sup>24,74–81</sup> (ESI, Fig. S10<sup>†</sup>) and by amperometric measurement (ESI, Fig. S11<sup>†</sup>) following a previous procedure established by us.<sup>24</sup> Griess assay measures the accumulation of nitrite and nitrate in water due to the rapid oxidation of NO in aerobic conditions, while amperometric



measurement measures the instantaneous release of NO. The media employed to determine the NO release can affect the measurement as demonstrated by Schoenfisch's group<sup>82</sup> and Reynolds' group.<sup>77,82</sup> For this reason, we decided to perform the release in phosphate buffer, which has been demonstrated to give more accurate results.

As indicated in Fig. 4 (and ESI, Fig. S10 and S11†), both tests showed a prolonged release of NO for several hours. Interestingly, NO released from GEN-NO nanoparticles followed first

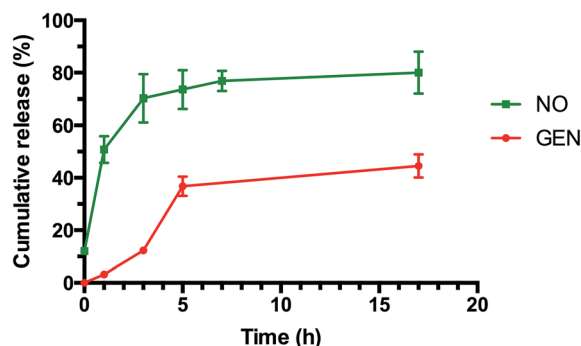


Fig. 4 Cumulative release of NO and GEN from GEN-NO nanoparticles at pH 7.4, 37 °C. The concentration of GEN-NO nanoparticles was 5 mg mL<sup>-1</sup>; experiments were performed in triplicate (the points represent the average of three values).

order kinetics that had a half-life of approximately 1 h at pH 7.4. After 5 h, over 75% of NO was released from the polymeric nanoparticles according to Griess assay (Fig. 4). Amperometric measurement (ESI, Fig. S11†) showed a rapid release of NO as the beginning of the experiment, which is consistent with Griess assay (*i.e.* approximately 10% of NO has been released after 10 min). More importantly, amperometric experiment showed a continuous release of NO for over 3.5 h. After 3.5 h, we added a free radical scavenger, *i.e.* 2-phenyl-4,4,5,5-tetramethylimidazole-1-oxyl-3-oxide (PTIO), into the vial in order to confirm that the amperometric signals being observed were due to NO. The signal of NO rapidly decreased after addition of PTIO. Interestingly, the encapsulation of NONOate in the core of nanoparticles appeared to enhance the stability of NONOate. Indeed, NONOate compounds such as diethylamine NONOate and spermine NONOate have very short half-lives (*i.e.* few minutes) as NONOates can spontaneously decompose to release NO in the presence of water.<sup>83</sup> This relative slow release is desirable for our application to achieve a long dispersion of biofilms and avoid a rapid reformation of biofilm, which allows the gentamicin to kill bacteria.

#### POEGMA-*b*-PVBA-gentamicin-NONOate eradicates *P. aeruginosa* biofilms

To evaluate the effect of the new POEGMA-*b*-PVBA-gentamicin-NONOate (GEN-NO nanoparticles) on biofilms, we first tested

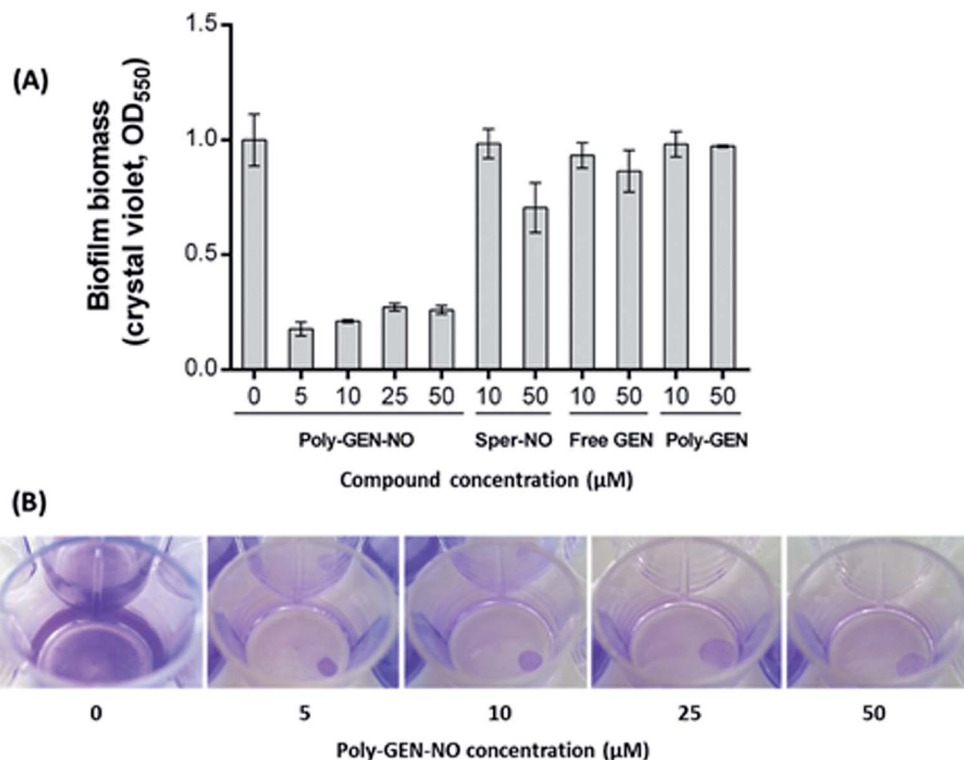


Fig. 5 GEN-NO nanoparticles induced dispersal in *P. aeruginosa* biofilms. (A) Bacterial biofilms were grown in multi-well plates for 6 h in the absence of any treatment before being treated for a further 1 h with various concentrations (μM) of NO donor spermine NONOate (Sper-NO), free gentamicin or gentamicin-conjugated polymers (Poly-GEN) and GEN-NO nanoparticles (Poly-GEN-NO). Biofilm biomass was analyzed by crystal violet staining. Error bars represent standard error ( $n = 2$ ). (B) Stained biofilms treated with the indicated concentrations of GEN-NO nanoparticles. Note: concentration based on GEN, one mole of GEN-NO nanoparticles is equivalent to one mole of Sper-NO and gentamicin.



their ability to release NO and disperse biofilms. Pre-established biofilms of the opportunistic pathogen and model biofilm-forming organism *P. aeruginosa* that had been grown for 6 h in the absence of any treatment, were treated with various compounds: (i) NO donor, spermine NONOate (Sper-NO); (ii) free GEN; (iii) gentamicin-conjugated polymers (Poly-GEN) and (iv) GEN-NO nanoparticles (Poly-GEN-NO). After 1 h treatment, the GEN-NO nanoparticles at 5  $\mu\text{M}$  (based on GEN, one mole of GEN-NO nanoparticles is equivalent to one mole of Sper-NO and gentamicin) were found to induce biofilm dispersal, leading to 83% reduction in biofilm biomass as determined by crystal violet (CV) staining, compared with untreated control biofilms (Fig. 5). Increasing the nanoparticle concentrations to 10–50  $\mu\text{M}$  (based on GEN), while still clearly inducing biofilm dispersal, resulted in slightly higher levels of staining on the well surfaces, which was possibly due to a higher amount of cells that were killed but not dispersed and thus also stained with CV. The addition of the NO donor, Sper-NO, which was used at equimolar concentrations compared to GEN-NO nanoparticles, led to only 30% reduction in biomass at 50  $\mu\text{M}$  (Fig. 5). This result is comparable to other NONOate-conjugated polymers that were previously shown to disperse biofilms.<sup>28,48</sup> Treatment with the antibiotic gentamicin alone only induced a small decrease in biofilm biomass at high concentrations, with 50  $\mu\text{M}$  free gentamicin leading to less than 14% reduction. Gentamicin-conjugated polymers (*i.e.* without NO) did not reduce the amount of cells attached on the surface at all concentrations tested (Fig. 5).

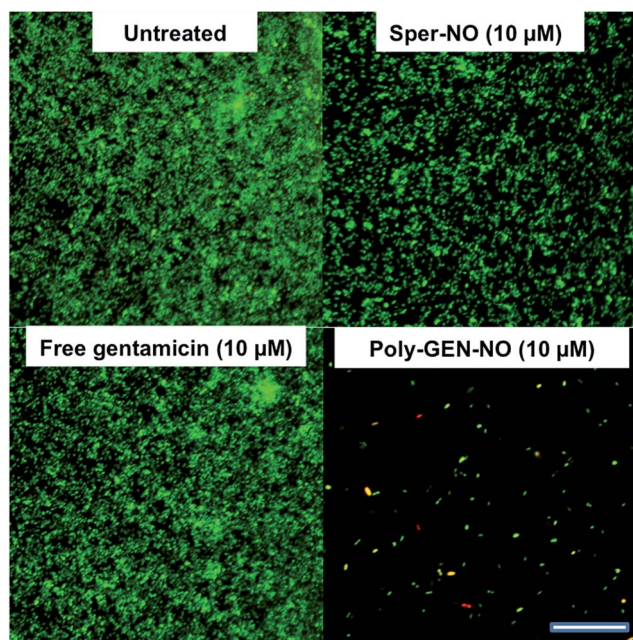


Fig. 6 Representative confocal images showing *P. aeruginosa* biofilms stained with LIVE/DEAD kit. Biofilms were grown for 6 h and then treated with NO donor spermine NONOate (Sper-NO), free gentamicin, GEN-NO nanoparticles or left untreated for a further 1 h before staining. Viable and non-viable bacteria appear green and red, as well as those stained both green/red, respectively. Scale bar = 50  $\mu\text{m}$ . Note: concentration based on GEN, one mole of GEN-NO nanoparticles is equivalent to one mole of Sper-NO and gentamicin.

Furthermore, confocal microscopy was used to evaluate the ability of the GEN-NO nanoparticles to disperse biofilms. Biofilm cells were stained with LIVE/DEAD dyes, where live and dead cells appear green and red, respectively. Cultures treated with GEN-NO nanoparticles at 10  $\mu\text{M}$  displayed greatly reduced biofilm biovolume and exhibited more dead cells, compared with untreated control biofilms or those inoculated with the NO donor or gentamicin alone (Fig. 6). Overall, the crystal violet and confocal microscopy results confirmed that GEN-NO nanoparticles were able to release NO, which was made available to biofilms, and consequently, induced dispersal of biofilm cells.

Next, the bactericidal properties of GEN-NO nanoparticles were investigated. *P. aeruginosa* biofilms were grown *in vitro* for 6 h as described above before being exposed to various treatments, including the NO donor, free GEN and GEN-NO nanoparticles. Then instead of analyzing the biofilm cultures by crystal violet staining, which can only account for total biomass, the viability of the cultures was assessed by measuring the ATP content of both biofilm and planktonic cells (Fig. 7). After 1 h treatment, a strong killing effect was observed in cell cultures treated with GEN-NO nanoparticles at 5–50  $\mu\text{M}$ , compared with the untreated control, free gentamicin or NO donor alone. At 10  $\mu\text{M}$ , GEN-NO nanoparticles almost completely eradicated both biofilm and planktonic cells. The viability of bacteria decreased

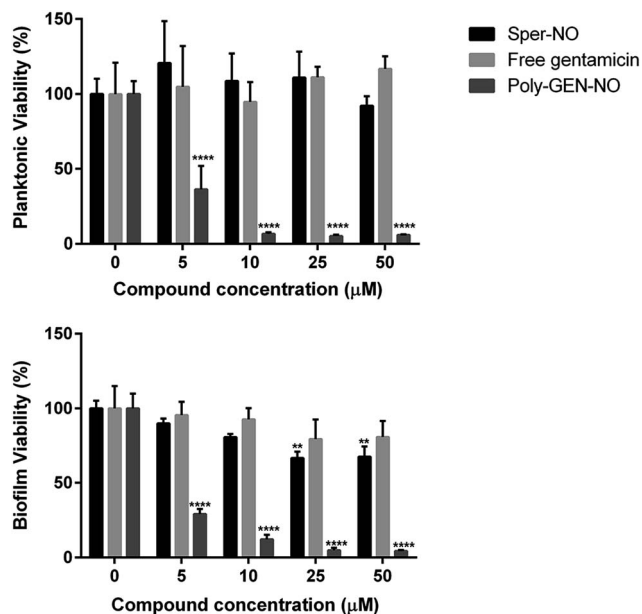


Fig. 7 Effect of GEN-NO nanoparticles on *P. aeruginosa* viability after combined release of NO and gentamicin. *P. aeruginosa* biofilms were grown in multi-well plates for 6 h in the absence of any treatments and treated further for 1 h in the presence of 5–50  $\mu\text{M}$  the NO donor spermine NONOate (Sper-NO), free gentamicin and GEN-NO nanoparticles (Poly-GEN-NO) before analyzing planktonic (top) and biofilm (bottom) viability by measuring the ATP content of bacteria. Error bars represent standard error ( $n = 4$ ). Asterisks indicate statistically significant difference of treatments versus untreated culture (\*\*,  $P < 0.01$ ; \*\*\*,  $P < 0.0001$ ). Note: concentration based on GEN, one mole of GEN-NO nanoparticles is equivalent to one mole of Sper-NO and gentamicin.





- 25 S. L. Chua, Y. Liu, J. K. Yam, Y. Chen, R. M. Vejborg, B. G. Tan, S. Kjelleberg, T. Tolker-Nielsen, M. Givskov and L. Yang, *Nat. Commun.*, 2014, **5**, 4462.
- 26 L. D. Christensen, M. van Gennip, M. T. Rybtke, H. Wu, W. C. Chiang, M. Alhede, N. Hoiby, T. E. Nielsen, M. Givskov and T. Tolker-Nielsen, *Infect. Immun.*, 2013, **81**, 2705–2713.
- 27 N. Barraud, M. J. Kelso, S. A. Rice and S. Kjelleberg, *Curr. Pharm. Des.*, 2015, **21**, 31–42.
- 28 H. T. T. Duong, N. N. M. Adnan, N. Barraud, J. S. Basuki, S. K. Kutty, K. Jung, N. Kumar, T. P. Davis and C. Boyer, *J. Mater. Chem. B*, 2014, **2**, 5003–5011.
- 29 H. T. T. Duong, Z. M. Kamarudin, R. B. Erlich, Y. Li, M. W. Jones, M. Kavallaris, C. Boyer and T. P. Davis, *Chem. Commun.*, 2013, **49**, 4190–4192.
- 30 B. Bonavida, S. Baritaki, S. Huerta-Yepepe, M. I. Vega, D. Chatterjee and K. Yeung, *Nitric Oxide*, 2008, **19**, 152–157.
- 31 A. Bratasz, N. M. Weir, N. L. Parinandi, J. L. Zweier, R. Sridhar, L. J. Ignarro and P. Kuppusamy, *Proc. Natl. Acad. Sci. U. S. A.*, 2006, **103**, 3914–3919.
- 32 Y. Lu, D. L. Slomberg, A. Shah and M. H. Schoenfish, *Biomacromolecules*, 2013, **14**, 3589–3598.
- 33 Y. Lu, D. L. Slomberg and M. H. Schoenfish, *Biomaterials*, 2014, **35**, 1716–1724.
- 34 D. A. Riccio and M. H. Schoenfish, *Chem. Soc. Rev.*, 2012, **41**, 3731–3741.
- 35 H. Zhang, G. M. Annich, J. Miskulin, K. Stankiewicz, K. Osterholzer, S. I. Merz, R. H. Bartlett and M. E. Meyerhoff, *J. Am. Chem. Soc.*, 2003, **125**, 5015–5024.
- 36 Y. Li, H. T. T. Duong, S. Laurent, A. MacMillan, R. M. Whan, L. V. Elst, R. N. Muller, J. Hu, A. Lowe, C. Boyer and T. P. Davis, *Adv. Healthcare Mater.*, 2015, **4**, 148–156.
- 37 S. Duan, S. Cai, Y. Xie, T. Bagby, S. Ren and M. L. Forrest, *J. Polym. Sci., Part A: Polym. Chem.*, 2012, **50**, 2715–2724.
- 38 S. Duan, S. Cai, Q. Yang and M. L. Forrest, *Biomaterials*, 2012, **33**, 3243–3253.
- 39 H. T. T. Duong, A. Ho, T. P. Davis and C. Boyer, *J. Polym. Sci., Part A: Polym. Chem.*, 2014, **52**, 2099–2103.
- 40 N. R. Yepuri, N. Barraud, N. Shah Mohammadi, B. G. Kardak, S. Kjelleberg, S. A. Rice and M. J. Kelso, *Chem. Commun.*, 2013, **49**, 4791–4793.
- 41 S. K. Kutty, N. Barraud, A. Pham, G. Iskander, S. A. Rice, D. S. Black and N. Kumar, *J. Med. Chem.*, 2013, **56**, 9517–9529.
- 42 T. Sun, Y. S. Zhang, B. Pang, D. C. Hyun, M. Yang and Y. Xia, *Angew. Chem., Int. Ed.*, 2014, **53**, 12320–12364.
- 43 D. Peer, J. M. Karp, S. Hong, O. C. Farokhzad, R. Margalit and R. Langer, *Nat. Nanotechnol.*, 2007, **2**, 751–760.
- 44 G. M. Whitesides, *Nat. Biotechnol.*, 2003, **21**, 1161–1165.
- 45 M. Ferrari, *Nat. Rev. Cancer*, 2005, **5**, 161–171.
- 46 Y. Lu, A. Shah, R. A. Hunter, R. J. Soto and M. H. Schoenfish, *Acta Biomater.*, 2015, **12**, 62–69.
- 47 E. M. Hetrick and M. H. Schoenfish, *Chem. Soc. Rev.*, 2006, **35**, 780–789.
- 48 H. T. Duong, K. Jung, S. K. Kutty, S. Agustina, N. N. Adnan, J. S. Basuki, N. Kumar, T. P. Davis, N. Barraud and C. Boyer, *Biomacromolecules*, 2014, **15**, 2583–2589.
- 49 D. L. Slomberg, Y. Lu, A. D. Broadnax, R. A. Hunter, A. W. Carpenter and M. H. Schoenfish, *ACS Appl. Mater. Interfaces*, 2013, **5**, 9322–9329.
- 50 E. M. Hetrick, J. H. Shin, N. A. Stasko, C. B. Johnson, D. A. Wespe, E. Holmuamedov and M. H. Schoenfish, *ACS Nano*, 2008, **2**, 235–246.
- 51 A. W. Carpenter and M. H. Schoenfish, *Chem. Soc. Rev.*, 2012, **41**, 3742–3752.
- 52 A. W. Carpenter, D. L. Slomberg, K. S. Rao and M. H. Schoenfish, *ACS Nano*, 2011, **5**, 7235–7244.
- 53 Y. Lu, D. L. Slomberg, B. Sun and M. H. Schoenfish, *Small*, 2013, **9**, 2189–2198.
- 54 P. N. Coneski and M. H. Schoenfish, *Chem. Soc. Rev.*, 2012, **41**, 3753–3758.
- 55 B. V. Worley, K. M. Schilly and M. H. Schoenfish, *Mol. Pharmaceutics*, 2015, **12**, 1573–1583.
- 56 B. V. Worley, D. L. Slomberg and M. H. Schoenfish, *Bioconjugate Chem.*, 2014, **25**, 918–927.
- 57 Y. Mitsukami, M. S. Donovan, A. B. Lowe and C. L. McCormick, *Macromolecules*, 2001, **34**, 2248–2256.
- 58 N. Barraud, J. A. Moscoso, J. M. Ghigo and A. Filloux, in *Pseudomonas Methods and Protocols*, ed. A. Filloux and J. L. Ramos, Humana Press, New York, NY, 2014, vol. 1149.
- 59 C. M. Maragos, D. Morley, D. A. Wink, T. M. Dunams, J. E. Saavedra, A. Hoffman, A. A. Bove, L. Isaac, J. A. Hrabie and L. K. Keefer, *J. Med. Chem.*, 1991, **34**, 3242–3247.
- 60 L. K. Keefer, R. W. Nims, K. M. Davies and D. A. Wink, in *Methods Enzymol.*, ed. P. Lester, Academic Press: 1996, vol. 268, pp. 281–293.
- 61 X. Chen, H. Hirt, Y. Li, S.-U. Gorr and C. Aparicio, *PLoS One*, 2014, **9**, e111579.
- 62 S. Mukherjee, A. P. Bapat, M. R. Hill and B. S. Sumerlin, *Polym. Chem.*, 2014, **5**, 6923–6931.
- 63 J. Liu, H. Duong, M. R. Whittaker, T. P. Davis and C. Boyer, *Macromol. Rapid Commun.*, 2012, **33**, 760–766.
- 64 A. W. Jackson and D. A. Fulton, *Chem. Commun.*, 2011, **47**, 6807–6809.
- 65 A. W. Jackson, C. Stakes and D. A. Fulton, *Polym. Chem.*, 2011, **2**, 2500–2511.
- 66 A. W. Jackson and D. A. Fulton, *Polym. Chem.*, 2013, **4**, 31–45.
- 67 H.-S. Lee, S. S. Dastgheyb, N. J. Hickok, D. M. Eckmann and R. J. Composto, *Biomacromolecules*, 2015, **16**, 650–659.
- 68 J. M. Vroom, K. J. de Grauw, H. C. Gerritsen, D. J. Bradshaw, P. D. Marsh, G. K. Watson, J. J. Birmingham and C. Allison, *Appl. Environ. Microbiol.*, 1999, **65**, 3502–3511.
- 69 A. P. Bapat, D. Roy, J. G. Ray, D. A. Savin and B. S. Sumerlin, *J. Am. Chem. Soc.*, 2011, **133**, 19832–19838.
- 70 A. P. Bapat, J. G. Ray, D. A. Savin, E. A. Hoff, D. L. Patton and B. S. Sumerlin, *Polym. Chem.*, 2012, **3**, 3112–3120.
- 71 A. P. Bapat, J. G. Ray, D. A. Savin and B. S. Sumerlin, *Macromolecules*, 2013, **46**, 2188–2198.
- 72 R. Ferrero, F. Rodríguez-Pascual, M. T. Miras-Portugal and M. Torres, *Br. J. Pharmacol.*, 1999, **127**, 779–787.
- 73 A. Hošťacká, I. Čižnár and M. Štefkovičová, *Folia Microbiol.*, 2010, **55**, 75–78.
- 74 Y. Li and P. I. Lee, *Mol. Pharmaceutics*, 2010, **7**, 254–266.



- 75 B. J. Heilman, J. St. John, S. R. J. Oliver and P. K. Mascharak, *J. Am. Chem. Soc.*, 2012, **134**, 11573–11582.
- 76 J. Sun, X. Zhang, M. Broderick and H. Fein, *Sensors*, 2003, **3**, 276.
- 77 J. L. Harding and M. M. Reynolds, *Anal. Chem.*, 2014, **86**, 2025–2032.
- 78 C. Vogt, Q. Xing, W. He, B. Li, M. C. Frost and F. Zhao, *Biomacromolecules*, 2013, **14**, 2521–2530.
- 79 K. S. Bohl and J. L. West, *Biomaterials*, 2000, **21**, 2273–2278.
- 80 K. A. Mowery, M. H. Schoenfisch, J. E. Saavedra, L. K. Keefer and M. E. Meyerhoff, *Biomaterials*, 2000, **21**, 9–21.
- 81 A. B. Seabra, R. da Silva and M. G. de Oliveira, *Biomacromolecules*, 2005, **6**, 2512–2520.
- 82 R. A. Hunter, W. L. Storm, P. N. Coneski and M. H. Schoenfisch, *Anal. Chem.*, 2013, **85**, 1957–1963.
- 83 L. K. Keefer, *ACS Chem. Biol.*, 2011, **6**, 1147–1155.
- 84 T.-F. Mah, B. Pitts, B. Pellock, G. C. Walker, P. S. Stewart and G. A. O'Toole, *Nature*, 2003, **426**, 306–310.
- 85 S. M. Abdelghany, D. J. Quinn, R. J. Ingram, B. F. Gilmore, R. F. Donnelly, C. C. Taggart and C. J. Scott, *Int. J. Nanomed.*, 2012, **7**, 4053–4063.

